DOI: 10.1002/ejic.200901078

$H_2InB_5O_{10}$: A New Pentaborate Constructed from 2D Tetrahedrally Four-Connected Borate Layers and InO_6 Octahedra

Rihong Cong,[a] Tao Yang,[a] Hongmei Li,[a] Fuhui Liao,[a] Yingxia Wang,*[a] and Jianhua Lin*[a]

Keywords: Borates / Indium / X-ray diffraction / Network structures / Hydrogen bonds

$H_2InB_5O_{10}$, a new hydrated indium pentaborate, was prepared by the boric acid flux method and characterized by IR, solid-state ^{11}B MAS NMR and ^{1}H CRAMPS NMR spectroscopy. Its structure was determined by powder X-ray diffraction and refined by Rietveld analysis. $H_2InB_5O_{10}$ crystallizes in the monoclinic space group *C*2. The structure features a new 2D tetrahedrally four-connected borate network constructed from a new pentaborate fundamental building block, B_5O_{14}. The 2D borate network is formed by two 6^3 borate layers linked by additional BO_4 groups in a spiro-5 mode and then combines with InO_6 octahedra to give rise to the 3D structure of $H_2InB_5O_{10}$. The strong hydrogen bonds that cross-link oxygen atoms of additional BO_4 groups between the borate layers help to stabilize the borate network.

Introduction

Borates have been one of the active topics in materials science for decades, because of their excellent performances as nonlinear optical (NLO) and luminescent materials.[1–4] The synthesis of borates with a new type of structure, and as a consequence with interesting properties, has attracted considerable attention.[5–9] The structures of borates are complicated and diverse, since the B atom can form triangular BO_3 and tetrahedral BO_4 units with oxygen atoms. These two groups can form large boron–oxygen anions by sharing oxygen atoms, so that complicated ring, chain, sheet or 3D networks result. In the known borates, boron-rich compounds, i.e. polyborates, however, are relatively rare, especially for high-valent metal borates.[10–12] The small size and high valence imply high local charge accumulation in anhydrous polyborates, which may cause the instability of the structure at high temperature;[13] therefore, it is difficult to synthesize high-valent metal polyborates by conventional solid-state reactions. Recently, remarkable progress has been made in the synthesis of new polyborates by applying improved synthetic routes, such as hydrothermal synthesis[10,11] and boric acid flux methods.[12,14] For example, in the Ln_2O_3–B_2O_3 (Ln = rare earth) system,[15] only three kinds of borates, i.e. oxyborate,[16,17] orthoborate[18,19] and metaborate,[20] are obtained by traditional solid-state reactions. By using the boric acid flux method, hydrous polyborates, such as rare earth pentaborate, octaborate and nonaborate, have been obtained.[21,22] The dehydration of the hydrous polyborates at certain temperatures give rise to the corresponding anhydrous polyborates with intriguing structures, for instance, those of α- and β-LnB_5O_9.[21,22]

The performance of In^{3+} is similar to that of rare earth cations (Ln^{3+}) in many compounds, as they have the same charge and a comparable radius size. As an efficient cathodoluminescent material, $InBO_3$ is the only known binary indium borate.[23,24] It has a calcite-type structure, is isostructural to $LuBO_3$ and only contains isolated BO_3 groups. Here, we report a new hydrous indium pentaborate, $H_2InB_5O_{10}$, which was obtained by the boric acid flux method. $H_2InB_5O_{10}$ crystallizes in the monoclinic space group *C*2 and comprises alternatively stacked isolated InO_6 octahedra layers and 2D sandwiched double borate layers formed exclusively by BO_4 tetrahedra. The interesting structural feature is the existence of a new fundamental building block, B_5O_{14}, which adopts an unusual spiro-5 connection mode[25–27] and comprises corner-sharing double three-membered borate rings. This new hydrous indium pentaborate transforms to a new anhydrous indium pentaborate InB_5O_9 after dehydration.

Results and Discussions

Structure Determination

The powder diffraction data of $H_2InB_5O_{10}$ can readily be indexed by a monoclinic lattice with constants a = 4.377, b = 7.861, c = 8.592 Å and β = 104.23° by using the program PowderX.[28] According to the systematic absence of the re-

[a] College of Chemistry and Molecular Engineering, Beijing National Laboratory for Molecular Sciences, State Key Laboratory for Rare Earth Materials Chemistry and Applications, Peking University,
Beijing 100871, China
Fax: +86-10-6275-1708
E-mail: jhlin@pku.edu.cn
wangyx@pku.edu.cn

Supporting information for this article is available on the WWW under http://dx.doi.org/10.1002/ejic.200901078.

flections, the space groups are limited to *C*2, *Cm* and *C*2/*m*. The structure model was then established in the space group of *C*2, which led to a chemically reasonable solution.

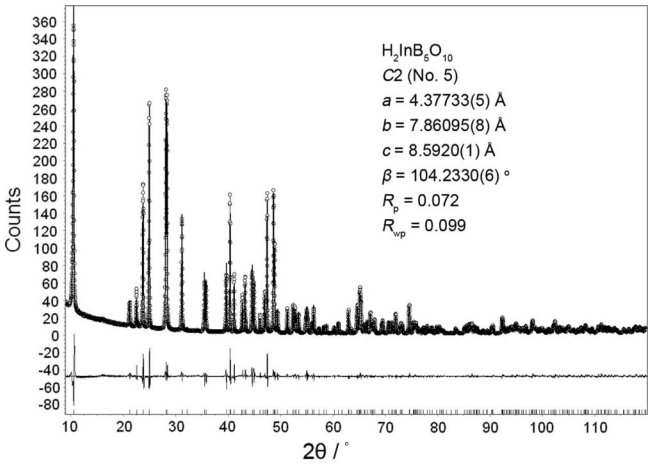

Figure 1. Observed, calculated and difference plots for Rietveld analysis of $H_2InB_5O_{10}$. The circles represent the observed data and the solid line is the calculated profile; the difference curve is shown below the diffraction profile, and the bars at the bottom are the Bragg reflection positions.

Table 1. Atomic coordinates and isotropic thermal displacement parameters of $H_2InB_5O_{10}$.

Atom	Wyckoff site	*x*	*y*	*z*	U_{eq} / Å^2	BVS
In	2*a*	0	0.3691	0	0.002(1)	2.78
B1	4*c*	0.895(5)	0.025(3)	0.783(3)	0.010(2)	3.16
B2	4*c*	0.393(5)	0.198(3)	0.770(3)	0.010(2)	2.89
B3	2*b*	0	0.626(2)	0.5	0.010(2)	2.96
O1	4*c*	0.355(2)	0.225(1)	0.604(1)	0.010(4)	1.71
O2	4*c*	0.745(2)	0.168(1)	0.847(1)	0.010(4)	1.85
O3	4*c*	0.3178(9)	0.365(3)	0.8454(5)	0.010(4)	1.98
O4	4*c*	0.223(2)	0.053(1)	0.821(1)	0.010(4)	2.03
O5	4*c*	0.751(1)	0.013(1)	0.604(1)	0.010(4)	1.48

Table 2. Selected distances [Å] and angles [°] for $H_2InB_5O_{10}$.

In–O3(×2)	2.147(4)	O2–In–O3	86.1(5)	O2–In–O4	84.8(5)
In–O2(×2)	2.18(1)	O2–In–O3	92.8(5)	O3–In–O4	96.2(5)
In–O4(×2)	2.24(1)	O2–In–O2	87.0(5)	O4–In–O4	99.5(5)
		O2–In–O3	92.8(5)	O2–In–O4	86.8(4)
		O2–In–O3	86.1(5)	O3–In–O4	96.2(5)
		O2–In–O4	86.8(4)	O3–In–O4	84.8(5)
B1–O4	1.41(2)	O3–B1–O4	111.5(16)	O2–B1–O5	108.6(12)
B1–O3	1.44(4)	O2–B1–O3	110.7(19)	O3–B1–O5	104.2(15)
B1–O2	1.48(3)	O2–B1–O4	108.4(16)	O4–B1–O5	113.4(16)
B1–O5	1.51(3)				
B2–O1	1.41(3)	O1–B2–O4	118.1(17)	O2–B2–O3	104.1(11)
B2–O4	1.49(3)	O2–B2–O4	106.1(15)	O3–B2–O4	110.8(13)
B2–O2	1.54(2)	O1–B2–O2	108.6(17)	O1–B2–O3	108.2(16)
B2–O3	1.54(3)				
B3–O1(×2)	1.446(9)	O1–B3–O1	115.2(7)	O5–B3–O5	108.3(6)
B3–O5(×2)	1.524(7)	O1–B3–O5	108.3(4)	O1–B3–O5	108.3(4)
		O1–B3–O5	108.3(4)	O1–B3–O5	108.3 (4)
		B1–O2–B2	116.4(11)	B1–O5–B3	128.2(11)
		B1–O3–B2	119.6(13)	B2–O1–B3	125.8(11)
		B1–O4–B2	127.1(13)		

The positions of all non-hydrogen atoms can be determined by the direct method with the program EXPO.[29,30] The structure was then refined by Rietveld analysis with the program TOPAS.[31] Soft restraints were applied to the thermal displacement parameters of the atoms. For the final refinement by the Rietveld method with TOPAS, the convergence values obtained for R_p and R_{wp} were 0.072 and 0.098, respectively, as shown in Figure 1. The atomic coordinates and selected bond lengths and angles are listed in Tables 1 and 2, respectively.

Crystal Structure of $H_2InB_5O_{10}$

There are nine crystallographically independent non-hydrogen atoms, one In, three B and five O atoms. The In and B3 atoms are located in a twofold axis (2*a* and 2*b* sites, respectively), and others are located in general positions. The indium atom is coordinated by six oxygen atoms in an octahedral environment with regular bond lengths and angles, and all the boron atoms are coordinated by four oxygen atoms in regular tetrahedral environments. The tetrahedral coordination of the boron atoms is confirmed by the solid-state ^{11}B MAS NMR result. As shown in Figure 2, the single peak at 0.5 ppm is related to the fourfold coordinated boron atoms.[32–35]

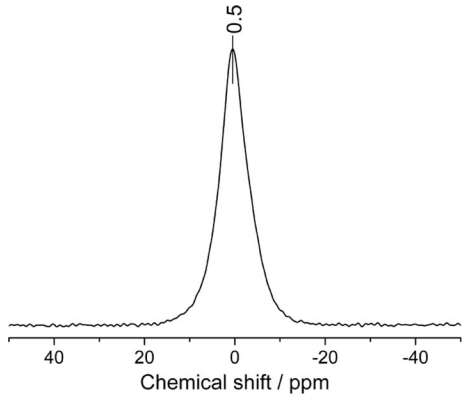

Figure 2. Solid-state ^{11}B MAS NMR spectrum of $H_2InB_5O_{10}$.

In borates, the fundamental building blocks (FBBs) concept is widely applied in describing the features of borate polyanions.[36–41] In $H_2InB_5O_{10}$, the FBB in the borate net is a pentaborate anion B_5O_{14}, which can be expressed as 5:[(5:5T)], as shown in Figure 3a. This pentaborate anion is formed by five BO_4 tetrahedra in a spiro-5 connection mode,[25–27] which is different from the three known pentaborate FBBs, 5:[(5:4Δ + T)], 5:[(5:3Δ + 2T)] and 5:[(5:2Δ + 3T)],[40,41] as shown in Figure 3b. The known pentaborate FBBs contain both triangular BO_3 and tetrahedral BO_4 groups in the form of a double three-ring (here, a six-membered ring made up of alternating boron and oxygen atoms, and the ring number only counts boron atoms) linked by a tetrahedral boron atom. From a structural view, trigonal BO_3 groups favour the formation of the three-ring, but BO_4

group may cause deformation of the ring. In FBB 5:[(5:2Δ + 3T)] (Figure 3b), for instance, the other two BO_4 groups are located on two sides to form two identical three-rings in the form of (Δ + 2T), instead of B_3O_5 (2Δ + T) and B_3O_9 (3T). It is well known that the tetrahedral borates are structurally similar to silicates that are built up on the basis of sharing oxygen atoms of tetrahedral SiO_4 groups. However, silicon seldom forms a three-ring with oxygen atoms alone because of the short Si–O bond length (≈1.61 Å) and large Si–O–Si angle (≈145°). Generally, the longer T–O (T is the centre atom in a tetrahedral environment) distance and relatively smaller T–O–T angle are necessary for the formation of three–ring (here T_3O_3-ring). It has been found that the incorporation of lower valent cations such as Al^{3+}, Be^{2+}, Zn^{2+} and even Li^+ can provide the necessary flexibility to stabilize the three-rings in tetrahedral frameworks.[25–27,42] The typical B–O bond length in tetrahedral borate groups is quite short (approximately 1.40–1.54 Å), which indicates that it should hinder formation of the three-ring. However, the lower charge of boron cation (+3) offsets this disadvantage. The weaker repulsion between two neighbouring B atoms enables the formation of the smaller B–O–B angle (with an approximate average value of 123°), which is advantageous to the formation of small rings, such as the three-ring. Three-ring B_3O_9 units have been observed in borates and borophosphates, for instance, $GdBO_3$ (low-temperature phase, LT phase),[43] $Ba_3B_6O_9(OH)_6$[44] and $BaBPO_5$.[45] In the structure of LT-$GdBO_3$, the three-ring B_3O_9 unit is isolated. In $Ba_3B_6O_9(OH)_6$, B_3O_9 rings connect with each other to form a helix chain (Figure S1a), with a hexaborate FBB unit, 6:[(5:5T) + (1:T)].[44] The three-ring chain in the structure of $BaBPO_5$ (Figure S1b) is similar to that of $Ba_3B_6O_9(OH)_6$, where half of the BO_4 groups are substituted by PO_4 groups.[45] To the best of our knowledge, 5:[(5:5T)] in $H_2InB_5O_{10}$ is the first pentaborate FBB that is constructed solely by BO_4 tetrahedra.

The pentaborate FBBs in $H_2InB_5O_{10}$ are connected to each other by sharing oxygen atoms, which form a two-dimensional sandwiched double layer, as shown in Figure 4a. The B–O–B angles within the FBB are marked in Figure 3a, and the other B–O–B angles in the borate layer are 116.4°, 119.6° and 127.1°, which are consistent with the data of known borates.[40] We can interpret the borate network in an alternative way. To focus on the monolayer of borates, it is clear that the BO_4 tetrahedra ($B1O_4$ and $B2O_4$) share three corners (O2, O3 and O4) to form a 6^3 net parallel to the *ab* plane, as shown in Figure 4b, and two 6^3 borate layers are linked by additional BO_4 ($B3O_4$) groups in a spiro-5 mode by sharing the fourth corners (O1 and O5 atoms) of $B1O_4$ and $B2O_4$, as shown in Figure 4a. The hexagonal arrangement of SiO_4 tetrahedra in a 6^3 net, with a composition of $[Si_2O_5]^{2-}$, is very common in silicates or aluminosilicates, such as $Li_2Si_2O_5$, $CaAl_2Si_2O_8$, talc, kaolinite etc.[46] In the single layer, each silicon atom is three-connected, leaving the fourth oxygen atom as a suspending group. The single layers can be linked together by cations, as in the structure of $Li_2Si_2O_5$, or combine with other structure blocks such as $Mg(OH)_2$ to form composite structures,

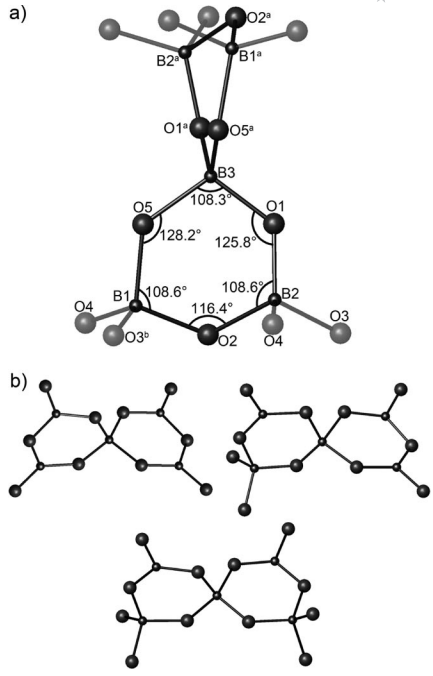

Figure 3. (a) Fundamental building block (FBB) in $H_2InB_5O_{10}$. Symmetry transformations used to generate equivalent atoms: [a]: $-x$, y, $-z$; [b]: $x + 1/2$, $y + 1/2$, z; (b) three known pentaborate FBBs, 5:[(5:4Δ + T)]; 5:[(5:3Δ + 2T)]; 5:[(5:2Δ + 3T)]. Small and large spheres represent B and O, respectively.

as in talc $Mg_3(OH)_2(Si_2O_5)_2$.[46] If the unshared vertices of all tetrahedra in a plane layer point to the same side of the layer, two layers can be combined to form a double layer by sharing the fourth vertexes, which means that the silicon atoms are all 4-connected. In this case, there must be partial replacement of Si by Al, such as $[Si_2Al_2O_8]^{2-}$, since otherwise the layer, which has the composition of SiO_2, would be neutral. In these structures, the double layer $[Si_2Al_2O_8]^{2-}$ is formed by directly sharing O atoms of two 6^3 layers. In the present study, the monolayer in $H_2InB_5O_{10}$ is the same as that in silicates, but the further connection of the layers into a double layer occurs in a different way. There is an array of additional BO_4 groups between the two monolayers, and these BO_4 groups link the two layers in spiro-5 modes to form a sandwiched double layer, as shown in Figure 4a. This 4-connected 2D network of the polyborate anion, with the formula $[B_5O_{10}]^{5-}$, is not only unique in borates, but is also the first to be observed in 4-connected networks.

The sandwiched double layers are further linked by In^{3+} in InO_6 octahedra, as shown in Figure 5. The two layers of the oxygen atoms (O2, O3 and O4) distribute in a distorted close packing manner, and the In^{3+} atoms locate in the octahedral holes formed by the oxygen atoms; the InO_6 block is related to CdI_2-type layer, but only 1/3 of the octahedral positions are occupied, as shown in Figure 5a. The occupation of In^{3+} cations can be elucidated by the structure of $Al(OH)_3$. In $Al(OH)_3$, the Al^{3+} ions occupy 2/3 of the octahedral positions and distribute in a honeycomb lattice. The

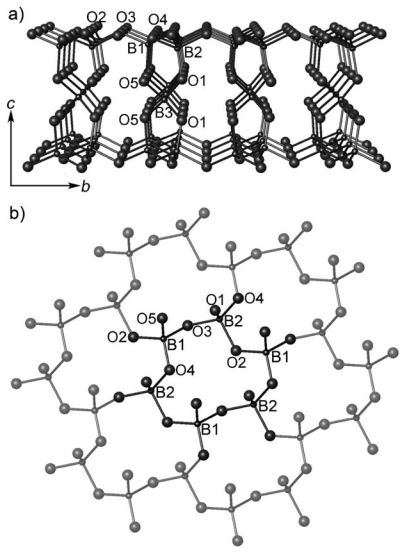

Figure 4. (a) 2D tetrahedrally 4-conneted sandwiched double borate layer in $H_2InB_5O_{10}$; (b) 6^3 borate network parallel to the *ab* plane. The six-ring borate is highlighted.

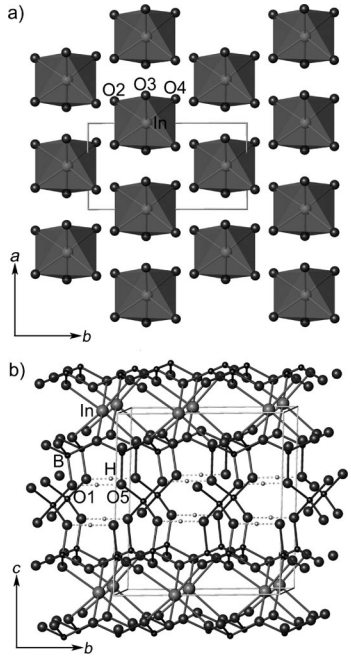

Figure 5. (a) Arrangement of the InO_6 octahedra in $H_2InB_5O_{10}$ with an opposite $Al(OH)_3$-type structure; (b) structural view of $H_2InB_5O_{10}$ along the [100] direction, and the hypothetical position of the hydrogen atom is at the midpoint between O1 and O5 (0.3030, 0.3688, 0.6041).

distribution of In^{3+} in $H_2InB_5O_{10}$ can be described as opposite to that of $Al(OH)_3$, where 1/3 of the empty octahedral positions in the structure of $Al(OH)_3$ are occupied by $In^{3+}$and the other 2/3 positions are empty. This results in the formation of isolated InO_6 octahedra in the structure. Since the radius of In^{3+} is quite large (0.81 Å), the occupation of In^{3+} ions in the octahedral positions swells the octahedral hole formed by the six oxygen atoms, and the distances between the oxygen atoms in the octahedron are much longer than those in octahedra without In^{3+} inside. Here, each oxygen atom connects to two BO_4 tetrahedra, which means that one InO_6 links to 12 BO_4 tetrahedra. The alternative stacking of the sandwiched double layer and In^{3+} ions gives rise to a 3D structure of the compound. A similar combination of metal-centred octahedra and sandwiched double borate layers was reported in $Bi_{0.96}$-$Al_{2.37}B_4O_{11}$,[47] as shown in Figure S2. However, in $Bi_{0.96}$-$Al_{2.37}B_4O_{11}$, the two monolayers are linked by disorderedly distributed AlO_5 units, where the Al^{3+} positions are half occupied, and additional oxygen atoms lie in the same layer as the Al^{3+} atoms.

If only non-hydrogen atoms are considered, the chemical formula of the structure can be written as $[InB_5O_{10}]^{2-}$. Apparently two hydrogen atoms are needed to compensate for the negative charges. It is difficult to identify the positions of the hydrogen atoms directly in the structure determination from powder X-ray diffraction data, but the summarization of bond valance for each oxygen atom is helpful for the location of the hydrogen atoms. The oxygen atoms in the structure can be classed into two groups: one includes O2, O3 and O4 atoms and the other includes O1 and O5 atoms. In the former group, each oxygen atom is connected to two B atoms and one In atom, and in the latter each oxygen atom is only connected to two B atoms. The BVS (bond valance sum) calculation reveals significantly low values for O1 and O5 (Table 2), which indicates the possible presence of protons attached to them. The distance between O1 and O5 is very short (2.31 Å), which reflects a very strong hydrogen bonding between them. According to a structurally reasonable analysis, we could locate a hydrogen atom in the position (0.3030, 0.3688, 0.6041), which is the midpoint between the O1 and O5 atoms, as shown in Figure 5b. The hydrogen bonding can further stabilize the 2D sandwiched double layer polyborate network. The solid-state ^1H CRAMPS NMR spectrum[48] of $H_2InB_5O_{10}$ shows a sharp peak at δ = 17.3 ppm (Figure 6a), which provides strong evidence for the existence of the very strong hydrogen bond.[49,50] Generally, the absorption band of the disengaged O–H stretching vibration is at about 3600 cm^{-1} in the IR spectrum. With the formation of hydrogen bonds, the absorption band shifts to lower wavenumbers and is accompanied by the broadening of the peak and weakening of the intensity.[51–53] The IR spectrum of $H_2InB_5O_{10}$ shows no absorption at about 3600 cm^{-1}, since the hydrogen bond in this compound is very strong (Figure 6b). One can suppose that the stretching vibration of O–H is "locked" by the very strong hydrogen bonds. There is a moderate broad absorption band at about 1200–1800 cm^{-1}, which might be related to the O–H vibration. The main peak at about 1500 cm^{-1} may be attributed to the bending vibration mode of the O–H group, and the shoulder peak at about 1700 cm^{-1} may be related to the stretching vibration of the O–H group in the strong hydrogen bond.[51–53] The vibration bands at about 1100 cm^{-1} are generally assigned to the vibration of the BO_4 groups.[54,55]

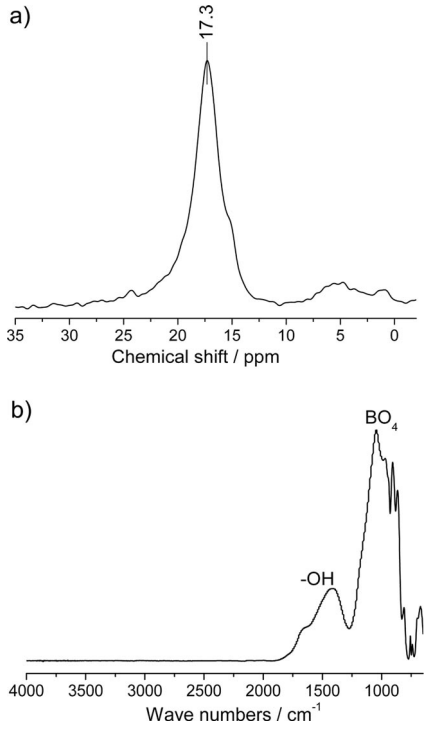

Figure 6. (a) Solid-state ^1H CRAMPS NMR spectrum and (b) IR spectrum of $H_2InB_5O_{10}$.

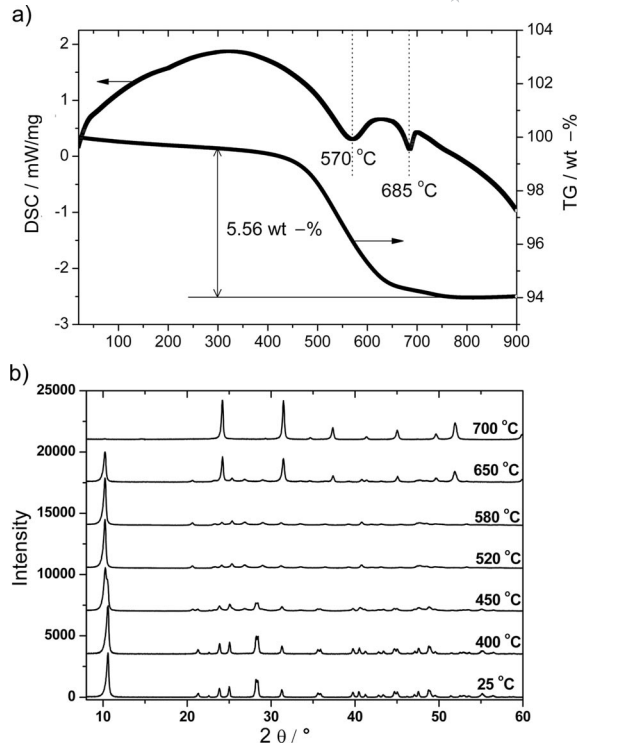

Figure 7. (a) TGA–DSC curves of $H_2InB_5O_{10}$; (b) X-ray diffraction patterns of the as-synthesized sample (25 °C) and its calcined products at different temperatures.

Thermal Behaviour of $H_2InB_5O_{10}$

The TGA-DSC curves of $H_2InB_5O_{10}$ are shown in Figure 7a. There are two endothermal peaks at about 570 °C and 685 °C in the DSC curve, and continuous weight loss (5.56 wt.-%) occurs between 400 and 700 °C in the TGA curve, which corresponds to the removal of one water molecule from the compound (calcd. 5.44 wt.-%). The thermal stability of the as-synthesized compound was also investigated by treating the sample at different temperatures. The powder X-ray diffraction profiles (Figure 7b) show that the structure is retained until 400 °C. At about 450 °C, it starts to dehydrate and this is accompanied by the appearance of a set of new reflections in the profile. These peaks can be assigned to the coexistence of $H_2InB_5O_{10}$ with its dehydration product InB_5O_9. The dehydration process is accompanied by an endothermal effect, which corresponds to the first peak in the DSC curve. With the increase in the temperature, the reflections for $H_2InB_5O_{10}$ disappear completely (520 °C and 580 °C), and the new profile corresponds to the dehydrated product:

$$H_2InB_5O_{10} \xrightarrow{450–580\ °C} InB_5O_9 + H_2O$$

The indexation of the new pattern gives a *C*-centred monoclinic lattice with a = 4.454(2), b = 7.680(4), c = 8.717(3) Å, β = 99.33(3)° and V = 1070.14 Å^3. In comparison with the lattice of the parent compound (a = 4.377, b = 7.861, c = 8.592 Å, β = 104.23°and V = 1084.90 Å^3), one can find that they have a close relationship, and the main framework may be maintained after dehydration. As shown in Figure 7b, the first peak (001) shifts to a lower angle in the dehydrated samples, which indicates an extension of the *c* axis, while the lengths of *a* and *b* both slightly shrink. The dehydration of $H_2InB_5O_{10}$ is accompanied by the removal of one oxygen atom, O1 or O5, which may result in a decrease in the coordination number of the related boron atoms and gives rise to BO_3 groups with a BO_3/BO_4 ratio of 2/3 in InB_5O_9. From the IR spectrum of InB_5O_9, we can identify that the absorption band of the BO_3 groups appear next to that of the BO_4 groups and that the intensity ratio of BO_4/BO_3 is approximately consistent with the hypothetical value (Figure S3). However, a detailed characterisation of the structure of InB_5O_9 has not yet been carried out because of the poor crystallization of the anhydrous product. An increase in the temperature leads to further decomposition. InB_5O_9 and $InBO_3$ coexist at 650 °C, and InB_5O_9 disappears completely at 700 °C (Figure 7b). This is accompanied by an endothermal effect, which corresponds to the second peak in the DSC curve (Figure 7a). According to the experimental results, it can be concluded that $H_2InB_5O_{10}$ starts to dehydrate at about 450 °C to form the anhydrous indium pentaborate InB_5O_9, which, as a medium phase, finally decomposes to $InBO_3$ and B_2O_3 at about 650 °C.

Conclusions

A new hydrated indium pentaborate $H_2InB_5O_{10}$ was synthesized by the boric acid flux method, and the structure was solved by powder X-ray diffraction. The structure of

$H_2InB_5O_{10}$ is constructed by the alternate stacking of 2D sandwiched double borate layers and InO_6 octahedra layers. The 2D borate network, which is formed solely by BO_4 tetrahedra, can be described as two monolayers with a 6^3 net interconnected by additional BO_4 in a spiro-5 manner. A new type of pentaborate fundamental building block (FBB), B_5O_{14}, was identified. This FBB, which consists of two corner-sharing double three-ring borates built by five BO_4 tetrahedra, is exactly the spiro-5 unit. The solid-state ^{11}B MAS NMR spectrum confirms the exclusive existence of the BO_4 tetrahedra in the structure. In the borate layer, there are hydrogen bonds that cross-link oxygen atoms of additional BO_4 groups, which help to stabilize the 2D borate network. The very strong hydrogen bonds are further confirmed by ^1H CRAMPS NMR spectroscopy. $H_2InB_5O_{10}$ transforms to its anhydrous pentaborate InB_5O_9 after dehydration at about 450 °C, and InB_5O_9 decomposes to $InBO_3$ and B_2O_3 at 650 °C.

Experimental Section

The starting materials, H_3BO_3 and In_2O_3, were of analytical grade and were used as purchased without further purification. Typically, 2.5 mmol In_2O_3 and H_3BO_3 with In/B ratios varying from 1:20 to 1:100 were charged into a 50-mL Teflon autoclave, which was then sealed in a steel vessel. The mixture was heated at 220–240 °C for 7–15 d and was then cooled to room temperature. The product was fully washed with hot water (80 °C) until the residual boric acid was completely removed. The title compound was obtained as a white powder, with a rough yield of 90%.

The chemical analysis of indium and boron was conducted by the ICP method on an ESCALAB2000 analyzer with a result of In/B ≈ 1:4.97, well consistent with the proposed formula. The thermal stability of $H_2InB_5O_{10}$ was analyzed by using combined thermogravimetric analysis (TGA) and differential scanning Calorimetry (DSC) on a Q600SDT Thermogravimetric Analyzer: the heating rate was 10 °C/min from 30 to 1000 °C under a nitrogen atmosphere. IR spectroscopy was measured on a NICOLET iN10 MX instrument. Solid-state ^{11}B MAS NMR and ^1H CRAMAP NMR spectroscopic data were recorded on a Varian Unity Plus-400 instrument with a 20-kHz spinning rate, with $BF_3{\cdot}OEt_2$ and $Si(CH_3)_4$ as standards, respectively.

Powder X-ray diffraction was performed on a Bruker D8 Advance diffractometer with monochromized Cu-$K_{\alpha1}$ radiation (λ = 1.540596 Å), and the data were collected by a PSD with open angle 2θ = 4° at room temperature in the 2θ range 8–120°, a step of 0.0144°, and a keeping time of 40 s for every step. The crystallographic data and the results of the Rietveld analysis are given in Table 3.

Table 3. Crystallographic data and Rietveld analysis results for $H_2InB_5O_{10}$.

Formula	$H_2InB_5O_{10}$
Formula weight / g mol^{-1}	330.89
Crystal system	monoclinic
Space group	$C2$
a / Å	4.37733(5)
b / Å	7.86095(8)
c / Å	8.5920(1)
β / °	104.2330(6)
V / Å^3	286.575(5)
Z	2
$\rho_{calcd.}$ / g cm^{-3}	3.836
λ / Å	1.540596
R_p	0.072
R_{wp}	0.098

Further details on the crystal structure investigations may be obtained from the Fachinformationszentrum Karlsruhe, 76344 Eggenstein-Leopoldshafen, Germany [Fax: (+49)7247-808-666; E-mail: crysdata@fiz-karlsruhe.de], on quoting the depository number CSD-421149.

Supporting Information (see footnote on the first page of this article): Borate chains in $Ba_3B_6O_9(OH)_6$ and $BaBPO_5$, the structure of $Bi_{0.96}Al_{2.37}B_4O_{11}$ and the IR spectrum of InB_5O_9 are presented.

Acknowledgments

This work was supported by the National Natural Science Foundation of China.

[1] P. Becker, *Adv. Mater.* **1998**, *10*, 979–992.
[2] H. Hellwig, J. Liebertz, L. Bohaty, *Solid State Commun.* **1998**, *109*, 249–251.
[3] A. Meijerink, J. Nuyten, G. Blasse, *J. Lumin.* **1989**, *44*, 19–31.
[4] C. R. Ronda, *J. Alloys Compd.* **1995**, *225*, 534–538.
[5] C. T. Chen, Y. B. Wang, B. C. Wu, K. C. Wu, W. L. Zeng, L. H. Yu, *Nature* **1995**, *373*, 322–324.
[6] D. M. Schubert, F. Alam, M. Z. Visi, C. B. Knobler, *Chem. Mater.* **2003**, *15*, 866–871.
[7] Z. T. Yu, Z. Shi, Y. S. Jiang, H. M. Yuan, J. S. Chen, *Chem. Mater.* **2002**, *14*, 1314–1318.
[8] J. L. C. Rowsell, N. J. Taylor, L. F. Nazar, *J. Am. Chem. Soc.* **2002**, *124*, 6522–6523.
[9] H. Huppertz, B. von der Eltz, *J. Am. Chem. Soc.* **2002**, *124*, 9376–9377.
[10] A. G. Ivanova, E. L. Belokoneva, O. V. Dimitrova, N. N. Mochenova, *Russ. J. Inorg. Chem.* **2006**, *51*, 584–588.
[11] A. G. Ivanova, E. L. Belokoneva, O. V. Dimitrova, N. N. Mochenova, *Russ. J. Inorg. Chem.* **2006**, *51*, 862–868.
[12] L. Y. Li, G. B. Li, Y. X. Wang, F. H. Liao, J. H. Lin, *Chem. Mater.* **2005**, *17*, 4174–4180.
[13] N. I. Leonyuk, *J. Cryst. Growth* **1997**, *174*, 301–307.
[14] P. C. Lu, Y. X. Wang, J. H. Lin, L. P. You, *Chem. Commun.* **2001**, 1178–1179.
[15] E. M. Levin, C. R. Robbins, J. L. Warring, *J. Am. Chem. Soc.* **1961**, *83*, 87–91.
[16] J. H. Lin, M. Z. Su, K. Wurst, E. Schweda, *J. Solid State Chem.* **1996**, *126*, 287–291.
[17] J. H. Lin, S. Zhou, L. Q. Yang, G. Q. Yao, M. Z. Su, L. P. You, *J. Solid State Chem.* **1997**, *134*, 158–163.
[18] M. Ren, J. H. Lin, Y. Dong, L. Q. Yang, M. Z. Su, L. P. You, *Chem. Mater.* **1999**, *11*, 1576–1580.
[19] Z. Yang, M. Ren, J. H. Lin, M. Z. Su, Y. Tao, W. Wang, *Chem. J. Chin. Univ.* **2000**, *21*, 1339–1343 (Chinese).
[20] G. K. Abdullaev, K. S. Mamedov, G. G. Dzhafarov, *Kristallografiya* **1975**, *20*, 265–269.
[21] L. Y. Li, P. C. Lu, Y. Y. Wang, X. L. Jin, G. B. Li, Y. X. Wang, L. P. You, J. H. Lin, *Chem. Mater.* **2002**, *14*, 4963–4968.
[22] L. Y. Li, X. L. Jin, G. B. Li, Y. X. Wang, F. H. Liao, G. Q. Yao, J. H. Lin, *Chem. Mater.* **2003**, *15*, 2253–2260.
[23] N. G. Kononova, A. E. Kokh, P. P. Fedorov, E. A. Tkachenko, *Neorg. Mater.* **2004**, *40*, 1373–1375; *Inorg. Mater. (Engl. Transl.)* **2004**, *40*, 1208–1210.
[24] J. R. Cox, D. A. Keszler, *Acta Crystallogr., Sect. C: Cryst. Struct. Commun.* **1994**, *50*, 1857–1859.
[25] S. Merlino, *Eur. J. Mineral.* **1990**, *2*, 809–817.
[26] M. J. Annen, M. E. Davis, J. B. Higgins, J. L. Schlenker, *J. Chem. Soc., Chem. Commun.* **1991**, 1175–1176.

[27] C. Röhrig, H. Gies, *Angew. Chem. Int. Ed. Engl.* **1995**, *34*, 63–65.
[28] C. Dong, *J. Appl. Crystallogr.* **1999**, *32*, 838–838.
[29] A. Altomare, G. Cascarano, C. Giacovazzo, A. Guagliardi, M. C. Burla, G. Polidori, M. Camalli, *J. Appl. Crystallogr.* **1994**, *27*, 1045–1050.
[30] A. Altomare, M. C. Burla, G. Cascarano, C. Giacovazzo, A. Guagliardi, A. G. G. Moliterni, G. Polidori, *J. Appl. Crystallogr.* **1995**, *28*, 842–846.
[31] *TOPAS V2.1: General Profile and Structure Analysis Software for Powder Diffraction Data*, Bruker AXS, Karlsruhe, Germany, **2002**.
[32] J. Li, S. P. Xia, S. Y. Gao, *Spectrochim. Acta* **1995**, *51*, 519–532.
[33] J. D. Epping, W. Strojek, H. Eckert, *Phys. Chem. Chem. Phys.* **2005**, *7*, 2384–2389.
[34] J. C. C. Chan, M. Bertmer, H. Eckert, *J. Am. Chem. Soc.* **1999**, *121*, 5238–5248.
[35] J. C. C. Chan, M. Bertmer, H. Eckert, *Chem. Phys. Lett.* **1998**, *292*, 154–160.
[36] C. L. Christ, J. R. Clark, *Phys. Chem. Miner.* **1977**, *2*, 59–87.
[37] P. C. Burns, J. D. Grice, F. C. Hawthorne, *Can. Mineral.* **1995**, *22*, 1131–1151.
[38] P. C. Burns, *Can. Mineral.* **1995**, *22*, 1167–1176.
[39] J. D. Grice, P. C. Burns, F. C. Hawthorne, *Can. Mineral.* **1999**, *37*, 731–762.
[40] G. H. Yuan, D. F. Xue, *Acta Crystallogr., Sect. B: Struct. Sci.* **2007**, *63*, 353–362.
[41] M. Touboul, N. Penin, G. Nowogrocki, *Solid State Sci.* **2003**, *5*, 1327–1342.
[42] C. Baerlocher, L. B. McCusker, D. H. Olson, *Atlas of Zeolite Framework Types, 6th Revised Edition*, Elsevier, New York, **2007**.
[43] M. Ren, J. H. Lin, Y. Dong, L. Q. Yang, M. Z. Su, *Chem. Mater.* **1999**, *11*, 1576–1580.
[44] Z. T. Yu, Z. Shi, Y. S. Jiang, H. M. Yuan, J. S. Chen, *J. Chem. Soc., Dalton Trans.* **2002**, 2031–2035.
[45] D. Y. Pushcharovsky, E. R. Gobetchia, M. Pasero, S. Merlino, O. V. Dimitrova, *J. Alloys Compd.* **2002**, *339*, 70–75.
[46] A. F. Wells, *Structural Inorganic Chemistry, 4th ed.*, Clarendon Press, Oxford, **1975**.
[47] A. V. Egorysheva, A. S. Kanishcheva, Yu. F. Kargin, Yu. N. Mikhailov, V. M. Skorikov, *Russ. J. Inorg. Chem.* **2007**, *52*, 58–61.
[48] B. H. Li, L. Xu, Q. Wu, T. H. Chen, P. C. Sun, Q. H. Jin, D. T. Ding, X. L. Wang, G. Xue, A. C. Shi, *Macromolecules* **2007**, *40*, 5776–5786.
[49] E. A. Johnson, G. R. Rossman, *Phys. Chem. Minerals* **2004**, *31*, 115–121.
[50] X. Y. Xue, M. Kanzaki, H. Fukui, E. Ito, T. Hashimoto, *Am. Miner.* **2006**, *91*, 850–861.
[51] A. N. Richard, O. K. Ronald, *Infrared Spectra of Inorganic Compounds*, Academic Press, New York, **1971**.
[52] V. M. F. Hammer, E. Libowitzky, G. R. Rossman, *Am. Miner.* **1998**, *83*, 569–576.
[53] E. Libowitzky, *Monatsh. Chem.* **1999**, *130*, 1047–1059.
[54] J. P. Laperches, P. Tarte, *Spectrochim. Acta* **1966**, *22*, 1201–1210.
[55] J. H. Denning, S. D. Ross, *Spectrochim. Acta* **1972**, *28A*, 1775–1785.

Received: November 5, 2009
Published Online: March 4, 2010

